240 KSME Journal, Vol. 9, No. 2, pp. 240~250, 1995

A High Resolution and Bounded Convection Scheme

Seok Ki Choi*, Ho Yun Nam* and Mann Cho*

(*Received August 28, 1994*)

A high resolution and bounded convection scheme is proposed for the simulation of steady incompressible flows with finite volume method. The scheme is formulated on a nonuniform, nonorthogonal grid so as to be applicable to the simulation of practical engineering problems. The relative performance of the scheme is evaluated through applications to the test problems. The results of numerical experiments show that the proposed scheme yields similiar solutions which are as good as those obtained with the QUICK scheme, but without exhibiting the physically unrealistic overshoots and undershoots.

Key Words : Finite Volume Method, Convection Scheme, Higher Order Bounded Scheme.

1. Introduction

Development of an efficient convection scheme which would simultaneously possess accuracy, stability, boundedness and algorithm simplicity has been one of the major tasks for the computational fluid dynamicists over the last two decades. Several different convection schemes have been proposed in the past, but there exists a conflicting issue of accuracy and boundedness among the schemes. The classical lower-order schemes such as the upwind scheme, the hybrid central/upwind [HYBRID] scheme and the power-law scheme (Patankar, 1980) are unconditionally bounded and highly stable but highly diffusive when the flow direction is skewed relative to the grid lines. Considerable efforts have been made toward the development of the improved differencing schemes, mainly in two directions. One is raising the order of the scheme and the other is taking into account the multidimensional nature of flow. The QUICK (Quardratic Upstream Interpolation for Convective Kinematics) scheme (Leonard, 1979) and the second-order upwind scheme (Warming and Beam, 1976) belong to the former approach and the skew-upwind scheme (Raithby, 1976) the latter. These schemes have been successful in increasing the accuracy of the solution, but all suffer from the boundedness problem, resulting in an oscillatory solution behaviour in regions of steep gradient, which can lead to the numerical instability.

Recently Gaskell and Lau(1988) developed a higher-order bounded scheme named SMART (Sharp and Monotonic Algorithm for Realistic Transport) employing a composite approach in which the high resolution schemes are combined with the lower-order bounded schemes. Leonard(1988) also proposed a similiar bounded scheme of third-order accuracy named SHARP(Simple High-Accuracy Resolution Program). These two schemes have resolved aforementioned boundedness problem without much deteriorating the accuracy of the higher-order scheme. However, numerical experiments (Zhu, 1992) have shown that these schemes need an underrelaxation treatment at each of the control volume cell faces in order to overcome the oscillatory convergence behaviours. This defficiency leads to the increase of the computer storage requirement, which may pose a practical constraint to their use in the complex three-dimensional turbulent flow calculations.

Subsequent studies by Zhu and Rodi (1991), Zhu(1991) and, Shin and Choi(1992) have proposed bounded convection schemes which are

*LMR Coolant Research Department, Korea Atomic Energy Research Institute, P.O. Box 105, Yousung, Daejon, 305-600, Korea

free of oscillatory convergence behaviours by choosing simple characteristics in the normalized variable diagram, such as a piecewise-linear profile (SOUCUP: Second-Order Upwind-Central differencing-first-order UPwind), a parabolic profile (HLPA: Hybrid Linear/Parabolic Approximation) and a cubic profile (SMARTER: SMART Efficiently Revised). These schemes are very simple to implement and computationally cost effective.

In the present study a high resolution and bounded convection scheme is proposed for the simulation of steady incompressible flows with finite volume method. The scheme employs a combination of piecewise linear characteristics in the normalized variable diagram. The scheme is formulated on a nonuniform, nonorthogonal grid so that it can be applicable to the practical engineering flow calculations. The performance of the scheme is tested through applications to the two-dimensional and three-dimensional test problems. The computed results are compared with the available benchmark solutions and experimental data. The results by the HYBRID, QUICK and SOUCUP schemes are also included for a better comparision with the existing popular schemes.

2. Mathematical Formulation

2.1 Governing equations

The conservation form of transport equation for a general dependent variable ϕ in a generalized coordinate system(ξ, η) can be written as follows:

$$\frac{\partial}{\partial\xi}(\rho U\phi)+\frac{\partial}{\partial\eta}(\rho V\phi) = \frac{\partial}{\partial\xi}\left[\frac{\Gamma_\phi}{J}\left(D_1^1\frac{\partial\phi}{\partial\xi}+D_2^1\frac{\partial\phi}{\partial\eta}\right)\right] + \frac{\partial}{\partial\eta}\left[\frac{\Gamma_\phi}{J}\left(D_1^2\frac{\partial\phi}{\partial\xi}+D_2^2\frac{\partial\phi}{\partial\eta}\right)\right]+JS_\phi \quad (1)$$

where

$$U=b_1^1u+b_2^1v,\quad V=b_1^2u+b_2^2v \quad (2)$$

and

$$b_1^1=y_\eta,\ b_2^1=-x_\eta,\ b_1^2=-y_\xi,\ b_2^2=x_\xi$$
$$D_1^1=x_\eta^2+y_\eta^2,\ D_2^2=x_\xi^2+y_\xi^2$$
$$D_2^1=D_1^2=-(x_\xi x_\eta+y_\xi y_\eta)$$
$$J=x_\xi y_\eta-x_\eta y_\xi \quad (3)$$

In these equations, ρ is the density of fluid, Γ_ϕ is the diffusion coefficient of the varible ϕ, (u, v) are the Cartesian velocity components in (x, y) directions and S_ϕ denotes the source term of the variable ϕ.

2.2 Discretization of transport equations

In the finite volume approach, the general transport equation, Eq. (1), is integrated over a control volume shown in Fig. 1. The resulting equation can be written as follow;

$$F_e-F_\omega+F_n-F_s=S_\phi\Delta V+S_\phi^b \quad (4)$$

where F represents the total flux of ϕ across the cell face and S_ϕ^b is the sum of the nonorthogonal diffusion terms. The total flux at the west face, for example, can be written as follows with the diffusion term approximated by the central differencing scheme.

$$F_\omega=(\rho U)_\omega\phi_\omega-\left(\frac{\Gamma_\phi}{J}D_1^1\right)_\omega(\phi_P-\phi_W) \quad (5)$$

The evaluation of ϕ_ω plays a key role in determining the accuracy and the stability of numerical solutions. For example, the ϕ_ω is evaluated as follows when one uses the first-order upwind scheme.

$$\phi_\omega=U_\omega^+\phi_W+U_\omega^-\phi_P \quad (6)$$

where U_ω^+ and U_ω^- are the indicators of the local velocity direction such that

$$U_\omega^+=0.5(1+|U_\omega|/U_\omega),$$
$$U_\omega^-=1-U_\omega^+(U_\omega\neq 0) \quad (7)$$

Incorporation of Eq. (6) and Eq. (5) and similiar expressions for the other cell faces leads to following general difference equation.

$$A_P\phi_P=A_E\phi_E+A_W\phi_W+A_N\phi_N+A_S\phi_S+b_\phi \quad (8)$$

The details of implementatioin of the higher-order bounded schemes will be outlined in the following chapter.

3. Higher-Order Bounded Schemes

The current higher-order bounded schemes are based on the variable normalization by Leconard(1988) and the convection boundedness criterion by Gaskell and Lau(1988). Consider, without loss of generality, the west face of control volume. We introduce a normalized variable such that

$$\hat{\phi}=\frac{\phi-\phi_U}{\phi_D-\phi_U} \tag{9}$$

where the subscripts U and D denote the upstream and the downstream locations. Eq. (9) can be rewritten in terms of nodal point values;

$$\hat{\phi}=\frac{\phi-\phi_{WW}}{\phi_P-\phi_{WW}}U_\omega^+ +\frac{\phi-\phi_E}{\phi_W-\phi_E}U_\omega^- \tag{10}$$

Using above upwind biased normalized variable, the following four schemes can be written as follows;

Central Difference Scheme ;

$$\hat{\phi}_\omega=[(1-C_2)\hat{\phi}_W+C_2]U_\omega^+ +[C_2\hat{\phi}_P+(1-C_2)]U_\omega^- \tag{11}$$

First-order Upwind Scheme:

$$\hat{\phi}_\omega=\hat{\phi}_W U_\omega^+ +\hat{\phi}_P U_\omega^- \tag{12}$$

Second-Order Upwind Scheme:

$$\hat{\phi}_\omega=(1+C_1)\hat{\phi}_W U_\omega^+ +(1+C_3)\hat{\phi}_P U_\omega^- \tag{13}$$

QUICK Scheme:

$$\hat{\phi}_\omega=\left[(1+C_1)(1-C_2)\hat{\phi}_W + C_2\left(1-\frac{C_1(1-C_2)}{C_1+C_2}\right)\right]U_\omega^+ +\left[C_2(1+C_3)\hat{\phi}_P+(1-C_2)\left(1-\frac{C_2C_3}{1-C_2+C_3}\right)\right]U_\omega^- \tag{14}$$

where

$$C_1=\frac{\Delta X_W}{\Delta X_W+\Delta X_{WW}},\quad C_2=\frac{\Delta X_W}{\Delta X_W+\Delta X_P},\quad C_3=\frac{\Delta X_P}{\Delta X_P+\Delta X_E} \tag{15}$$

are the geometric interpolation factors definded in terms of the size of control volume cell. For example, ΔX_P is the size of control volume around the calculation point P and is defined as (see Fig. 1)

$$\Delta X_P=\overline{\omega P}+\overline{Pe} \tag{16}$$

The normalized diagrams for these well known schemes($U_\omega>0$) are shown in Fig. 2.

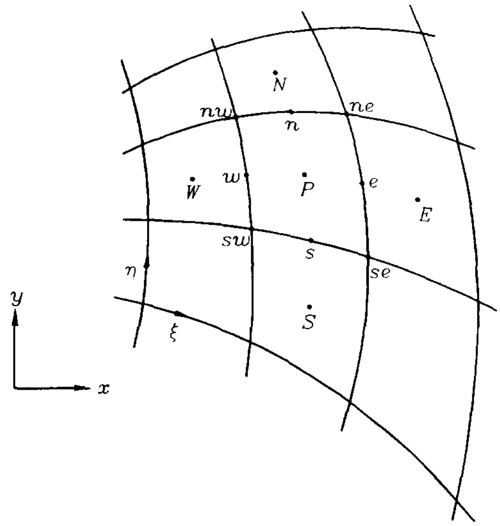

Fig. 1 A typical control volume

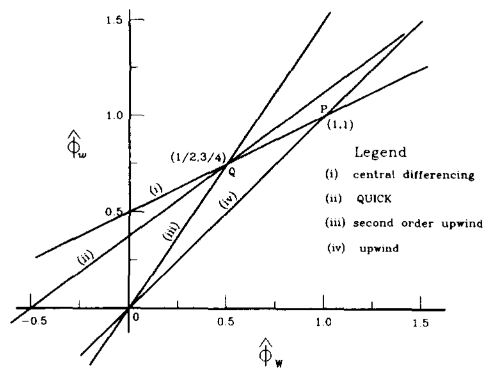

Fig. 2 The normalized variable diagram for various well known schemes

Gaskell and Lau (1988) formulated following convection boundedness criterion. Define a continuous increasing function or union of piecewise continuous increasing function F relating the modelled normalized face value $\hat{\phi}_\omega$ to the normalized upstream nodal value $\hat{\phi}_W$ ($U_\omega>0$), that is $\hat{\phi}_\omega=F(\hat{\phi}_W)$. Then a finite difference approximation to $\hat{\phi}_\omega$ is bounded if

i) for $0\leqq\hat{\phi}_W\leqq 1$, F is bounded below by the function $\hat{\phi}_\omega=\hat{\phi}_W$ and above by unity and passes through the points (0, 0) and (1, 1);

ii) for $\hat{\phi}_W<0$, $\hat{\phi}_W>1$, F is equal to $\hat{\phi}_W$.

The convection boundedness criterion is a neces-

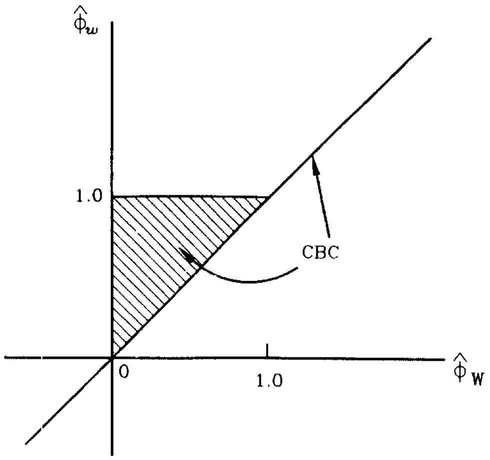

Fig. 3 Diagrammatic representation of the convection boundedness criterion

sary and sufficient condition for achieving computed boundedness if only three neighbouring nodal values are used to approximate the face values. The diagrammatic representation of the convection boundedness criterion is shown in Fig. 3.

According to Leonard (1988), for any (in general nonlinear) characteristics in the normalized variable diagram (Fig. 2),

i) passing through Q is necessary and sufficient for second-order accuracy

ii) passing through Q with a slope of 0.75(for a uniform grid) is necessary and sufficient for third-order accuracy.

The horizontal and vertical coordinates of point Q in the normalized variable diagram and the slope of the characteristics at the point Q for preserving the third-order accuracy for a nonuniform grid can be obtained by a simple algebra Eqs. (11)~(14).

$$X_Q=\frac{C_2}{C_1+C_2}U_\omega^+ +\frac{1-C_2}{1-C_2+C_3}U_\omega^-$$
$$Y_Q=\frac{C_2(1+C_1)}{C_1+C_2}U_\omega^+ +\frac{(1-C_2)(1+C_3)}{1-C_2+C_3}U_\omega^-$$
$$S_Q=(1+C_1)(1-C_2)U_\omega^+ + C_2(1+C_3)U_\omega^- \qquad (17)$$

For a uniform grid, $X_Q=0.5$, $Y_Q=0.75$ and $S_Q=0.75$.

Following above criteria by Gaskell and Lau (1988) and by Leonard (1988), one may choose several bounded characteristics in the normalized variable diagram whose order of accuracy is determined by the shape of the characteristics. Followings are two simple possibilites which ensure the second or third-order accuracy.

The SOUCUP scheme

The SOUCUP scheme (Zhu and Rodi, 1991) employs union of piecewise linear characteristics passing through the points, O, Q and P in the normalized variable diagram.

$$\hat{\phi}_\omega=\begin{cases} a_\omega+b_\omega\hat{\phi}_C & 0\leqq\hat{\phi}_C\leqq X_Q \\ c_\omega+d_\omega\hat{\phi}_C & X_Q\leqq\hat{\phi}_C\leqq 1 \\ \hat{\phi}_C & \text{otherwise} \end{cases} \qquad (18)$$

where

$$a_\omega=0$$
$$b_\omega=Y_Q/X_Q$$
$$c_\omega=(Y_Q-X_Q)/(1-X_Q)$$
$$d_\omega=(1-Y_Q)/(1-X_Q) \qquad (19)$$

and

$$\hat{\phi}_C=\hat{\phi}_W U_\omega^+ + \hat{\phi}_P U_\omega^- \qquad (20)$$

The SOUCUP scheme is a composite of second-order upwind, central differencing and first-order upwind scheme. We see that the SOUCUP scheme is second-order accurate according to the criterion by Leonard(1988).

The COPLA scheme

The order of accuracy of the scheme may be increased to the third-order if one introduces a characteristic curve in the normalized variable diagram whose slope at the interesction point Q is the same as that of the third-order accurate QUICK scheme. Such a scheme is proposed in the present study using following characteristics in the normalized variable diagram.

$$\hat{\phi}_\omega=\begin{cases} a_\omega+b_\omega\hat{\phi}_C & 0\leqq\hat{\phi}_C\leqq 0.5X_Q \\ c_\omega+d_\omega\hat{\phi}_C & 0.5X_Q\leqq\hat{\phi}_C\leqq 1.5X_Q \\ e_\omega+f_\omega\hat{\phi}_C & 1.5X_Q\leqq\hat{\phi}_C\leqq 1 \\ \hat{\phi}_C & \text{otherwise} \end{cases} \qquad (21)$$

where

$$a_\omega=0$$

$$b_\omega=(2Y_Q-S_QX_Q)/X_Q$$
$$c_\omega=Y_Q-S_QX_Q$$
$$d_\omega=S_Q$$
$$e_\omega=(3X_Q-2Y_Q-S_QX_Q)/(3X_Q-2)$$
$$f_\omega=(2Y_Q+S_QX_Q-2)/(3X_Q-2) \qquad (22)$$

The present COPLA (COmbination of Piecewise Linear Approximation) scheme employs a composite of piecewise linear characteristics in which the QUICK scheme is employed in a range of $0.5X_Q \leqq \hat{\phi}_C \leqq 1.5X_Q$. The scheme is similiar to the SMART scheme (Gaskell and Lau, 1988), but is free of convergence oscillation. The normalized variable diagrams for the SOUCUP scheme and the COPLA scheme are given in Fig. 4.

The implementation of the higher-order bounded schemes are quite simple. A part of Eq. (18) can be expressed in terms of the unnormalized variable.

$$\phi_\omega=\left\{\phi_W+(\phi_P-\phi_{WW})\left[a_\omega^+ +(b_\omega^+-1)\left(\frac{\phi_W-\phi_{WW}}{\phi_P-\phi_{WW}}\right)\right\}U_\omega^- + \left\{\phi_P+(\phi_W-\phi_E)\left[a_\omega^- +(b_\omega^--1)\left(\frac{\phi_P-\phi_E}{\phi_W-\phi_E}\right)\right\}U_\omega^- \qquad (23)$$

Given the switch factors,

for $U_\omega>0$,

$$a_\omega^+=1 \text{ if } |\phi_P-2\phi_W+\phi_{WW}|<|\phi_P-\phi_{WW}|$$
$$a_\omega^+=0 \quad \text{otherwise} \qquad (24)$$

for $U_\omega<0$,

$$a_\omega^-=1 \text{ if } |\phi_W-2\phi_P+\phi_E|<\phi_W-\phi_E|$$
$$a_\omega^-=0 \quad \text{otherwise} \qquad (25)$$

the unnormalized form of Eq. (23) can be rewritten as

$$\phi_\omega=U_\omega^+\phi_W+U_\omega^-\phi_P+\Delta\phi_\omega \qquad (26)$$

where

$$\Delta\phi_\omega=U_\omega^+a_\omega^+(\phi_P-\phi_{WW})\left[a_\omega^+ +(b_\omega^+-1)\left(\frac{\phi_W-\phi_{WW}}{\phi_P-\phi_{WW}}\right)\right]+U_\omega^-a_\omega^-(\phi_W-\phi_E)\left[a_\omega^- +(b_\omega^--1)\left(\frac{\phi_P-\phi_E}{\phi_W-\phi_E}\right)\right] \qquad (27)$$

After the evaluation of the additional term, the implementation of this scheme is the same as that of the first-order upwind scheme. It should be noted that the constants are switched according to the value of $\hat{\phi}_C$ at the same cell face and for the same flow direction. In the present study the additional terms are treated in a deferred correction way proposed by Khosla and Rubin(1974).

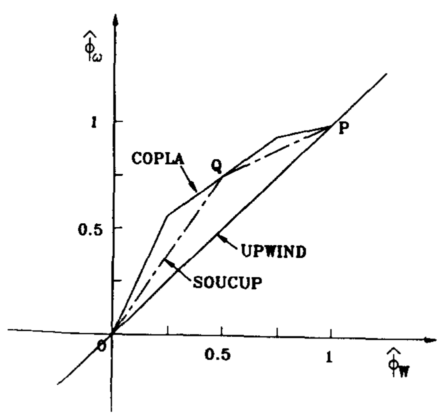

Fig. 4 The normalized variable diagram for SOUCUP and COPLA bounded schemes

4. Applications to Text Problems

The higher-order bounded schemes described in the previous chapter are implemented in a general purpose computer code designed to solve fluid flow and heat transfer in complex geometries. The computer code uses a nonstaggered grid arrangement and the SIMPLE (Patankar, 1980) algorithm for pressure-velocity coupling. The momentum interpolation practice by Rhie and Chow (1983) is employed for calculating the cell-face mass fluxes to avoid the pressure osillation.

The test problems include; (1) pure convection of a scalar variable in two different situations, (2) laminar flow in a lid-driven cavity with and without inclination, (3) laminar flow in a square duct of 90-degree bend. The computed results are compared with the analytic solution, the available experimental data and other computed results reported in the literature.

4.1 Pure convection of a scalar variable

In what follows, we present the results of two linear problems involving purely convective transport of scalar tracers containing discontinuties by prescribed velocity fields. They are; (1) pure convection of a scalar step by a uniform velocity field, (2) pure convection of a box-shaped scalar step by a uniform velocity field. These simple yet stringent test cases were extensively used in the literature to examine the performance of the convection schemes.

The flow configuration for Case-1 is shown in Fig. 5. Calculations are performed for two different flow angles, $\theta=45°$ and $\theta=26.6°$, employing 22*22 uniform grids. Fig. 6 shows the predicted profiles along the centerline by different convection schemes. It can be seen that the HYBRID scheme results in very diffusive profiles at both angles. Both accuracy and boundedness are achieved by the bounded schemes. The sharp gradient is fairly well resolved without introdcuing the supurious overshoots and undershoots. We can observe that the SOUCUP scheme is relatively more diffusive than the COPLA scheme. The QUICK scheme also fairly well resolves the steep gradient, but exhibits oscillatory behaviours. This oscillatory solution behaviour is a little sensitive to the orientation of the flow field. The magnitude of undershoot is more pronounced at a smaller flow angle($\theta=26.6°$).

As a second test problem of pure convection (Case-2), we consider a box-shaped profile shown in Fig. 7, which is generated by imposing a step profile along the bottom and left-hand walls of the square solution domain. Calculations are performed with two different meshes, 22*22 and 42*42. The predicted profiles along the vertical centerline ($x=0.5$, $0\leq y\leq 1$) are shown in Fig. 8. We can observe that the solutions by the

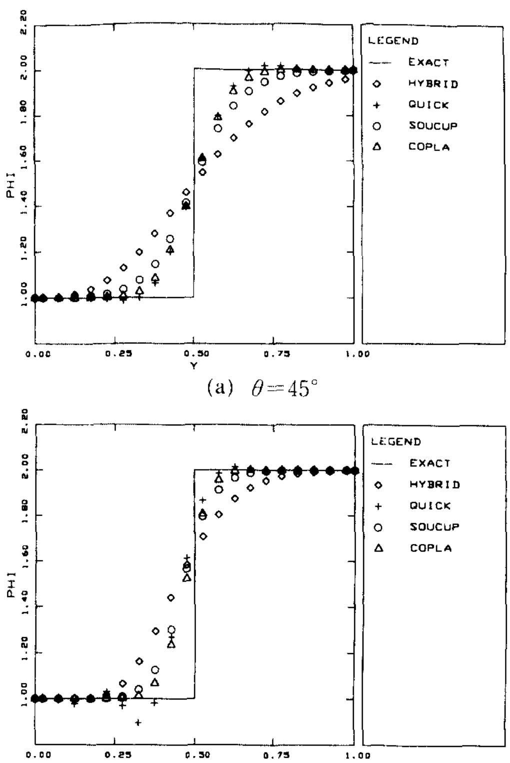

(a) $\theta=45°$

(b) $\theta=26.6°$

Fig. 6 ϕ-profile along the centerline

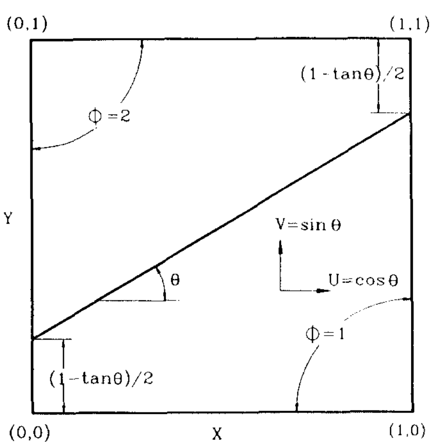

Fig. 5 Case-1 : Pure convection of a scalar step by a uniform velocity field

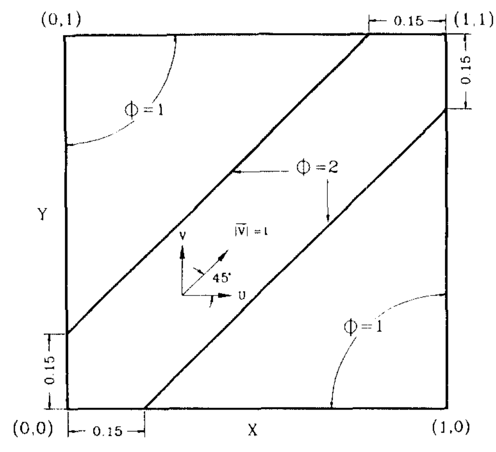

Fig. 7 Case-2 : Pure convection of a box-shaped scalar step by a uniform velocity field

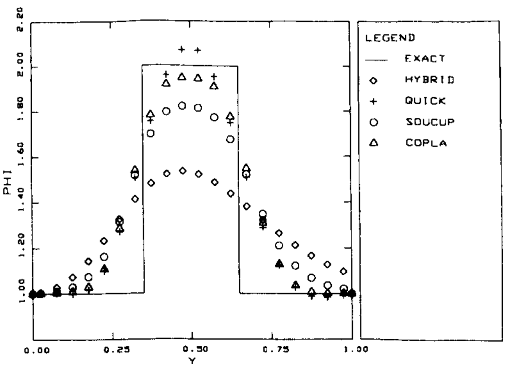

(a) 22*22 grid

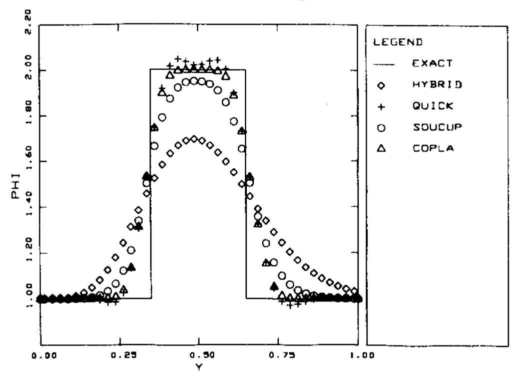

(b) 42*42 grid

Fig. 8 ϕ-profile along the centerline

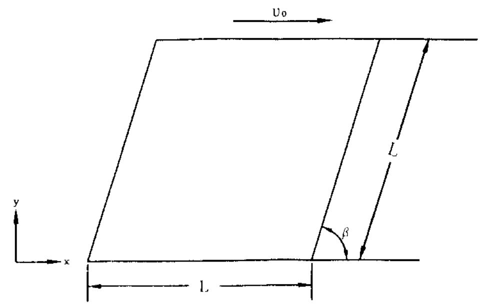

Fig. 9 Laminar flow in a lid-driven cavity

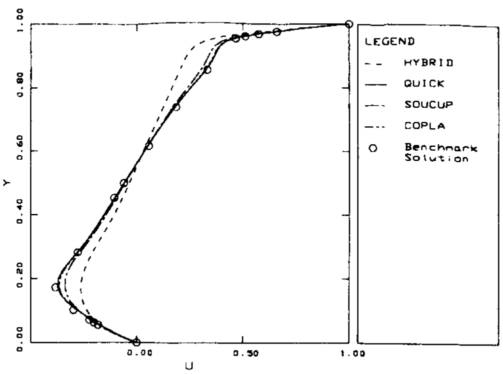

(a) $\beta=90°$

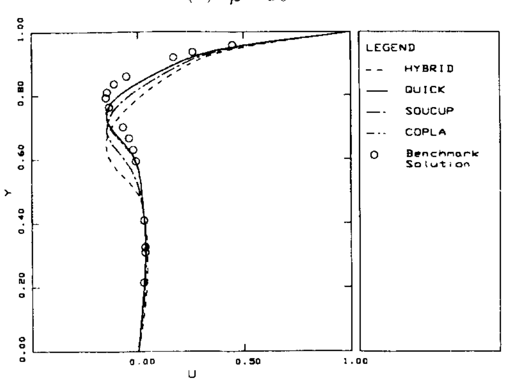

(b) $\beta=45°$

Fig. 10 Centerline u-velocity distributions

HYBRID scheme are very diffusive, even when the grids are increased by a facotor of two. The QUICK scheme results in severe overshoots when the grid is coarse (22*22), but shows relatively low undershoots. The bounded schemes fairly well resolve the steep gradient on either side of the peaked profile. The SOUCUP scheme is more diffusive than the COPLA scheme again, but is much better than the HYBRID scheme.

4.2 Laminar flow in a lid-driven cavity with and without inclination

Laminar flow in a lid-driven square cavity, schematically shown in Fig. 9, is considered as an example of nonlinear problems which are of practical interest. Two cases with different inclinations ($\beta=90°$, $\beta=45°$) are considered to examine the grid nonorthogonality effect on the solution behaviours. At present reliable benchmark solutions are available for both cases. Calculations are performed for Reynolds number of 1000 employing 42*42 numerical grids. The computed results are compared with the benchmark solutions by Ghia et al. (1982) ($\beta=90°$) and by Demirdzic et al. (1992) ($\beta=45°$).

The computed U-velocity profiles along the vertical centerline for both cases are presented in Fig. 10. For these recirculating type flow calculations, the QUICK scheme results in the most accarate solution. The results by the HYBRID scheme are too diffusive, questioning that this scheme can be applied to the complex three-dimensional flow calculations. We can observe that the COPLA scheme yields solutions which are as good as those obtained by the QUICK scheme. The SOUCUP scheme is again more diffusive than the COPLA scheme. The general solution behaviours among the different convection schemes are not altered with the change of the grid nonorthogonality.

4.3 Laminar flow in a square duct of 90-degree bend

Laminar flow in a square duct of 90-degree bend, schematically shown in Fig. 11, is considered in the present study as a typical three-dimensional flow involving a strong secondary

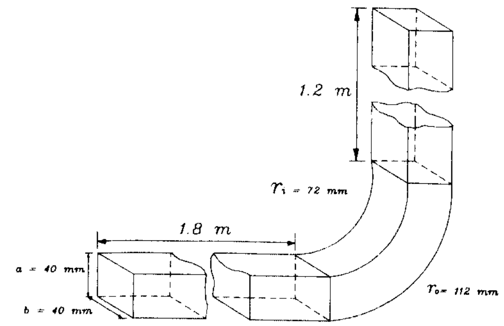

Fig. 11 Laminar flow in a square duct of 90-degree bend

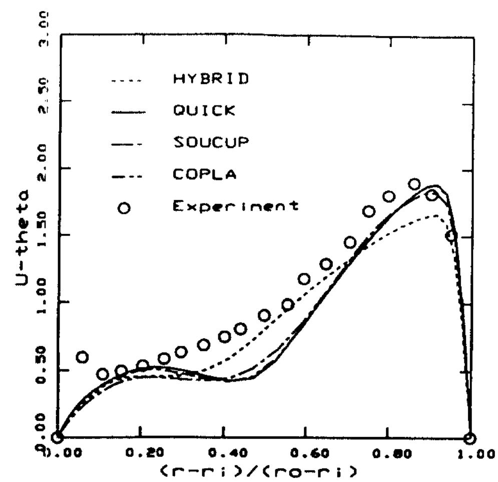

(a) 60-degree plane, z/b=0.5

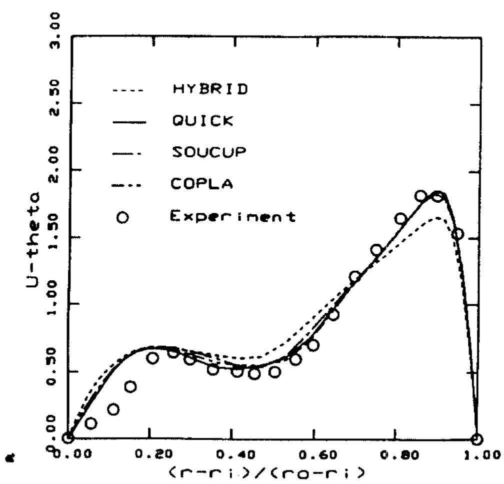

(c) 90-degree plane, z/b=0.5

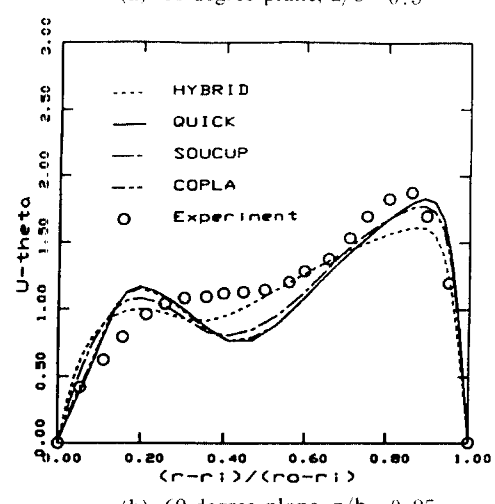

(b) 60-degree plane, z/b=0.25

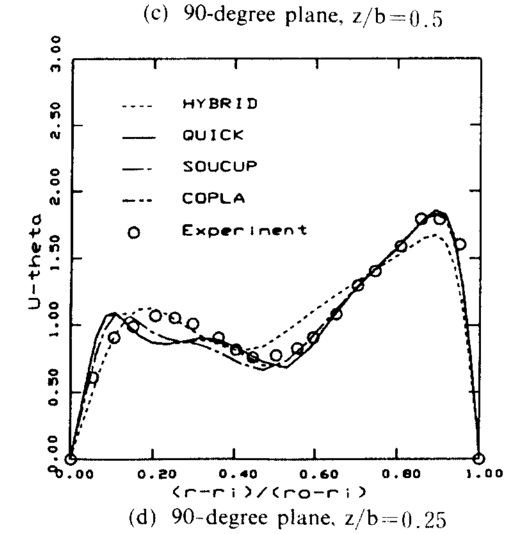

(d) 90-degree plane, z/b=0.25

Fig. 12 Predicted streamwise velocity profiles

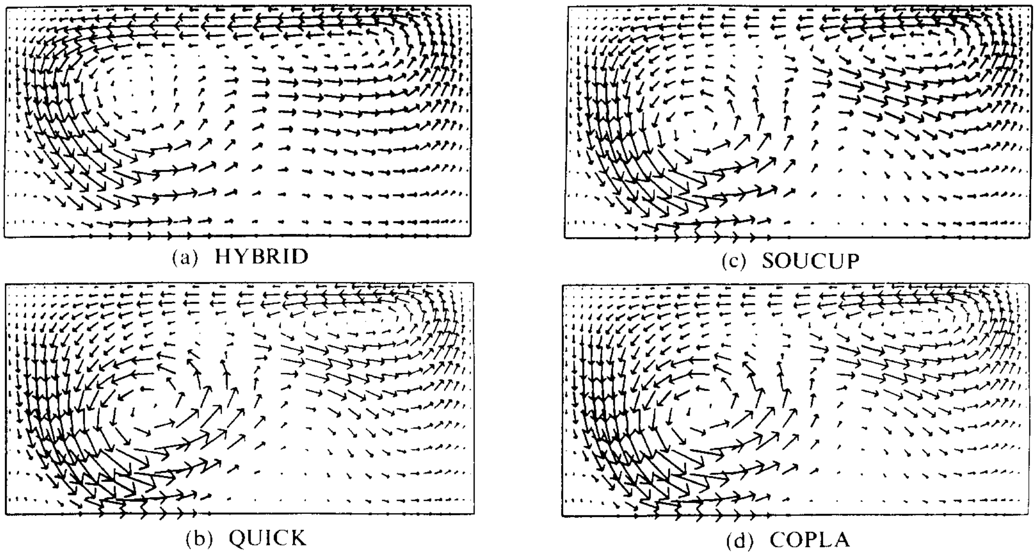

Fig. 13 Predicted secondary flow in the 90-degree plane

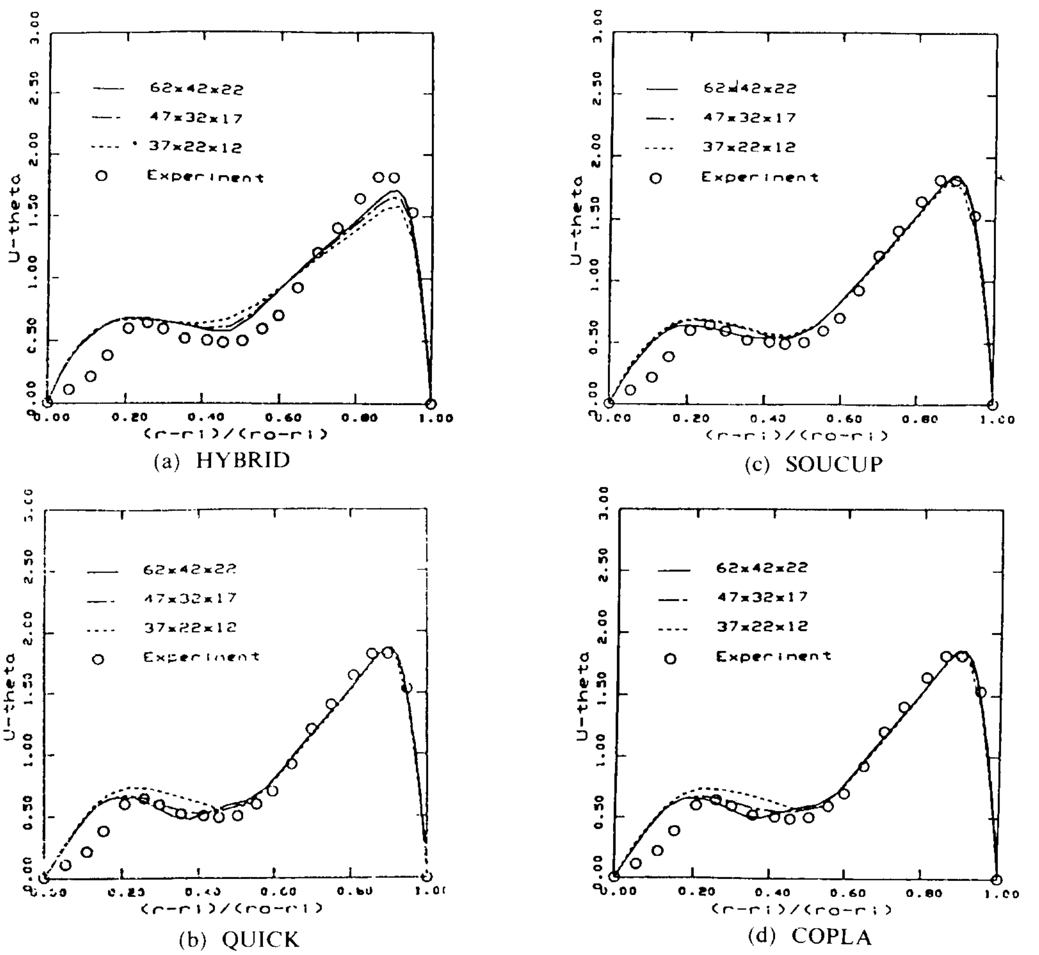

Fig. 14 Effect of grid refinement in the 90-degree symmetry plane

motion caused by the centrifugal force and pressure gradient. This particular problem was studied experimentally by Humphrey et al. (1977). The Reynolds number based on the hydraulic diameter and bulk velocity is 790. Only a symmetric half of the solution domain is solved employing 47*32*17 nonuniform grids.

Fig. 12 shows the predicted streamwise velocity profiles at the 90-degree and 60-degree planes together with the measured data. We note that the HYBRID scheme consistently results in diffusive solutions. Especially it underpredicts the peaked velocity profiles. The QUICK and COPLA schemes result in nearly the same solutions, while the SOUCUP scheme produces slightly more diffusive solutions than the QUICK or COPLA schemes.

Fig. 13 shows the vector plots of the predicted secondary flow at the 90-degree plane. The QUICK, COPLA and SOUCUP schemes result in nearly identical secondary flow features. The HYBRID scheme produces a slightly different result, especially the secondary motion near the symmetry line and the strength and the location of the primary vortex.

In order to investigate the effect of grid refinement on the solution, numerical experiments have been performed employing three different numerical grids (37*22*12, 47*32*17, 62*42*22). Fig. 14 shows their results at the 90-degree symmetry plane. The HYBRID solution is not grid independent and changes gradually as the grid is refined. The solutions by the higher-order schemes nearly reach the grid-independent solution. We can notice that the higher-order schemes well predict the peak velocity profiles. It is of interest to see that the coarsest QUICK solution is better than the finest HYBRID solution.

5. Conclusions

A high-resolution and bounded convection scheme which employs piecewise linear characteristics in the normalized variable diagram is proposed and tested through applications to two linear pure convection problems, and two and three-dimensional flow problems. The results of numerical experiments show that the proposed scheme resolves the boundedness problem retaining the accuracy of higher-order scheme. The scheme is simple to implement, stable and is free of convergence oscillation. All these desired features make the present scheme a good alternative to many existing schemes for the calculation of complex three-dimensional flow problems.

References

Demirdzic, I., Lilek, Z. and Peric, M., 1992. "Fluid Flow and Heat Transfer Test Problems for Non-Orthogonal Grids: Bench-Mark Solution," *Int. J. Numer. Methods Fluids,* Vol. 15, pp. 329 ~354.

Gaskell, P. H. and Lau, A. K. C., 1988, "Curvature-Compensated Convective Transport: SMART, A New Boundedness Preserving Transport Algorithm," *Int. J. Numer. Methods Fluids,* Vol. 8, pp. 617~641.

Ghia, U., Ghia, K. N. and Shin, C. T., 1982, "High-Re Solutions for Incompressible Flow Using the Navier-Stokes Equations and a Multigrid Method," *J. Comput. Physics,* Vol. 48, pp. 387~411.

Humphrey, J. A. C., Taylor, A. M. K. and Whitelaw, J. H., 1977, "Laminar Flow in a Square Duct of Strong Curvature," *J.F.M.,* Vol. 83, pp. 509~527.

Khosla, P. K. and Rubin, S. G., 1974, "A Diagonally Dominant Second-Order Accurate Implicit Scheme," *Comput. Fluids,* Vol. 2, pp. 207 ~209.

Leonard, B. P., 1979, "A Stable and Accurate Convective Modelling Procedure Based on Quadratic Interpolation," *Comput. Methods Appl. Mech. Engng.,* Vol. 19, pp. 59~98.

Leonard, B. P., 1988, "Simple High-Accuracy Resolution Program for Convective Modelling of Discontinuities," *Int. J. Numer. Methods Fluids,* Vol. 8, pp. 1291~1318.

Patankar, S. V., 1980, *Numerical Heat Transfer and Fluid Flow,* McGraw-Hill.

Raithby, G. D., "Skew Upstream Differencing Schemes for Problem Involving Fluid Flow," *Comput. Methods Appl. Mech. Engng.,* Vol. 9, pp. 153～164.

Rhie, C. M. and Chow, W. L., 1983, "Numerical Study of the Turbulent Flow Past an Airfoil with Trailing Edge Separtion," *AIAA J.*, Vol. 21, pp. 1525～1532.

Shin, J. K. and Choi, Y. D., 1992, "Study on the Improvement of the Convective Differencing Scheme for the High-Accuracy and Stable Resolution of the Numerical Solution," *Trans. KSME*, 16-6, pp. 1179～1194 (in Korea).

Warming, R. F. and Beam, R. M., 1976, "Upwind Second-Order Difference Schemes and Applications in Aerodynamic Flows," *AIAA J.*, Vol. 14, pp. 1241～1249.

Zhu, J., 1991, "A Low-Diffusive and Oscillation-Free Convection Scheme," *Comm. Appl. Numer, Methods*, Vol. 7, pp. 225～232.

Zhu, J., 1992, "On the Higher-Order Bounded Discretization Schemes for Finite Volume Computations of Incompressible Flow," *Comput. Methods Appl. Mech. Egng.*, Vol. 98, pp. 345～360.

Zhu, J. and Rodi, W., 1991, "A Low Dispersion and Bounded Convection Scheme," *Comput. Methods Appl. Mech. Engng.*, Vol. 92, pp. 225～232.